Improving Continuous-variable Quantum Channels with Unitary Averaging

S. Nibedita Swain,[1,2,3] Ryan J. Marshman,[3] Peter P. Rohde,[4]
Austin P. Lund,[3,5] Alexander S. Solntsev,[1] and Timothy C. Ralph[3]

[1] *School of Mathematical and Physical Sciences, University of Technology Sydney, Ultimo, NSW 2007, Australia*
[2] *Sydney Quantum Academy, Sydney, NSW 2000, Australia*
[3] *Centre for Quantum Computation and Communication Technology, School of Mathematics and Physics, University of Queensland, Brisbane, Queensland 4072, Australia*
[4] *BTQ & Centre for Engineered Quantum Systems, Macquarie University, Sydney NSW, Australia*
[5] *Xanadu, Toronto, Ontario, M5G 2C8, Canada*

(Dated: January 12, 2025)

A significant hurdle for quantum information and processing using bosonic systems is stochastic phase errors which occur as the photons propagate through a channel. These errors will reduce the purity of states passing through the channel and so reducing the channels capacity. We present a scheme of passive linear optical unitary averaging for protecting unknown Gaussian states transmitted through an optical channel. The scheme reduces the effect of phase noise on purity, squeezing and entanglement, thereby enhancing the channel via probabilistic error correcting protocol. The scheme is robust to loss and typically succeeds with high probability. We provide both numerical simulations and analytical approximations tailored for relevant parameters with the improvement of practical and current technology. We also show the asymptotic nature of the protocol, highlighting both current and future relevance.

I. INTRODUCTION

Optical quantum systems play a major role in a wide range of quantum technology applications offering distinct advantages [1]. Currently, some of the most developed and practical quantum information applications of optical systems are based on Gaussian source states [2] (such as squeezed states) and linear networks. Examples include continuous variable (CV) versions of teleportation [3] and quantum key distribution [4] as well as Gaussian Boson sampling [5–8]. However, in order to enable scalable quantum applications it is essential to establish practical approaches for controlling noise in these quantum optical systems. The non-universal nature of deterministic linear optics processing means standard approaches to error correction are not immediately applicable and other approaches need to be explored.

One such alternative approach is unitary averaging (UA) [9–12], a framework that has been shown to help reduce errors within discrete variable (DV) linear optical setups, i.e. set-ups in which non-Gaussian, single photon source states are injected into linear networks. It is not immediately obvious that UA can be usefully extended to systems with Gaussian inputs due to various Gaussian no-go theorems [13–15]. The role of vacuum projection with respect to the theorems is non-trivial. None-the-less we show that such an extension is possible and useful, leading to a powerful generalization of the UA technique.

To illustrate the effect we focus on a simple but practically relevant example: a single mode propagating through a channel with stochastic phase noise. Such a situation is generic in continuous variable quantum communication scenarios but might also be relevant in optical circuits due to fabrication variations or the incorporation of thermal components. Phase noise typically arises due to small fluctuations in path length/timing between the optical modes. This may be between the quantum modes themselves and/or the quantum modes and a reference mode (the local oscillator). It has long been known to limit squeezing strength [16] and can particularly be a problem in quantum communication protocols [17]. We characterise the improvement in the channel by analysing a two-mode squeezed vacuum state [18] with half the state sent through the channel. Previous techniques employed multiple copies of the input state to reduce phase noise [19–21]. In contrast, here a single copy of an unknown state is sent through multiple copies of the channel before being recombined non-deterministically. We demonstrate that Gaussian encoding with vacuum projection (as used for recombination) has strong utility for protecting Gaussian states against phase errors. This leads to a significant improvement in the purity, entanglement and squeezing through the averaged channel with a high probability of success. Importantly, the protocol continues to perform effectively in the presence of loss in the optical elements.

II. UNITARY AVERAGING ON DV SYSTEMS

In the UA framework, one utilises redundancy in the applied transformation, rather than redundant encoding to protect against errors. The success probability is known to depend on the variance in the individual unitaries. UA acts to apply an averaged unitary evolution [9, 10] on discrete variable (DV) systems given by

$$\hat{u} = \frac{1}{N}\sum_{k=1}^{N} \hat{U}_k \tag{1}$$

using N copies of the unitary. The choice of $\hat{u}$ over $\hat{U}$ signifies that the resulting transformation in DV systems

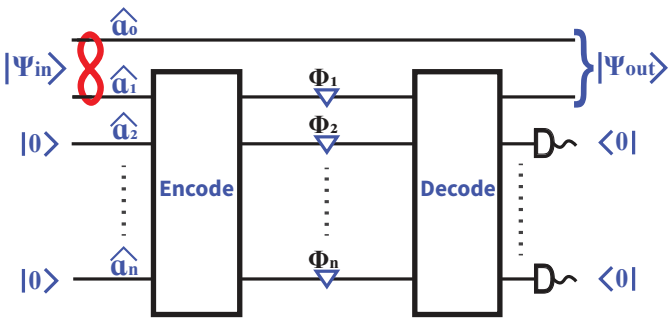

Figure 1: Scheme for passive unitary averaging. Redundant encoding using beamsplitter network for general n. One mode ($\hat{a}_1$) of a two mode squeezed vacuum state is input into the encoding network beam splitter network which evenly distributes the state across n copies of the transmission mode. Each mode applies an independent phase noise $\Delta\Phi_i$. The decoding network inverts the encoding circuits action and upon hearlding the $n-1$ error modes in the vacuum state, produces an output state with reduced noise.

is non-unitary. Additionally, there are a set of $(N-1)$ 'error' modes that are heralded by vacuum projections to signal the success of this transformation. This average transformation $\hat{u}$ represents a stochastic operator which approximates the target unitary with a variance reduced by a factor N [9]. For DV optics this was found to allow a trade-off between the transformation fidelity and the the heralded probability of success.

We will now apply UA to a single mode channel suffering stochastic phase noise.

III. PASSIVE UNITARY AVERAGING ON CV SYSTEMS

We will model the effect of UA on a CV system by considering a two-mode squeezed vacuum state [22, 23], with one mode fed through the noisy channel which is then characterised by the output squeezing, purity and entanglement. The two mode squeezed vacuum was chosen as it can model various types of input states through projective measurement. One arm of a two-mode squeezed state forms a Gaussian thermal state which can be decomposed into number state, coherent state or squeezed state bases (amongst others). These decompositions can be physically realised via photon number, heterodyne and homodyne projective measurements on the other arm, respectively. It is of no consequence whether the projections are made before or after the first arm is sent through the channel. Thus analysis of the properties of a two-mode squeezed state after one arm has passed through a channel provides general information about the characteristic of the channel. Fig.1 shows the circuit we will be considering. We direct one mode of the two-mode squeezed vacuum state into the interferometer, while leaving the other mode free. The encode and decode transformations consist of $50:50$ beamsplitters implementing a Hadamard transform to evenly mix all modes together. Finally, the $(n-1)$ output modes are heralded in the vacuum leaving the signal to be output through the final, undetected mode.

The input state is given by

$$|\psi_{\text{in}}\rangle = \hat{S}(r)\,|0\rangle\,|0\rangle \otimes |0\rangle^{\otimes(n-1)} \tag{2}$$

where the two-mode squeezing operator $\hat{S}(r)$ acts on only the first two modes

$$\hat{S}(r) = \exp\left[-r(\hat{a}_0\hat{a}_1 - \hat{a}_0^\dagger\hat{a}_1^\dagger)\right] \tag{3}$$

After passing through the interferometer and heralding vacuum in the last $(n-1)$ modes, the output state, Eq.2 is

$$\left(\otimes_{j=2}^{n}\langle 0|_j\right)\hat{U}\hat{S}(r)\,|0\rangle\,|0\rangle \otimes |0\rangle^{\otimes(n-1)} = |\psi_{\text{out}}\rangle \tag{4}$$

where $\hat{U} = (\hat{H}^\dagger * \hat{R}(\theta) * \hat{H})_{n\times n}$, $\hat{H}$ is the Hadamard transforms acting as the encoding and decoding circuits, and $\hat{R}(\theta)$ implements stochastic phase transformations on each mode, representing the noise. The output state is,

$$|\psi_{\text{out}}\rangle = (\cosh r)^{-1}\sum_N(-1)^j\left[\frac{e^{i\phi_1}+e^{i\phi_2}+...+e^{i\phi_n}}{n}\tanh r\right]^N|N,N\rangle \tag{5}$$

We will simplify this by defining

$$\alpha e^{i\phi_\beta} = \frac{e^{i\phi_1}+e^{i\phi_2}+...+e^{i\phi_n}}{n} \tag{6}$$

$$\tanh r' = \alpha\tanh r \tag{7}$$

The phase terms ϕ_j vary randomly and independently around some mean value. Hence, the output state after vacuum heralding is

$$|\psi_{out}\rangle = \frac{1}{\mathbf{N}}(\cosh r)^{-1}\sum_N(-1)^N[e^{i\phi_\beta}\tanh r']^N\,|N,N\rangle$$
$$= \hat{S}(\chi')\,|0\rangle\,|0\rangle \tag{8}$$

where $\mathbf{N}$ is a normalisation constant related to probability of success, and $\chi' = r'e^{i\phi_\beta}$.

The normalisation constant for the output state (5) is,

$$\mathbf{N} = \frac{\cosh r'}{\cosh r} \tag{9}$$

giving a probability of success $P = |\frac{\cosh r'}{\cosh r}|^2$.

While each individual use of the channel will produce two mode squeezed state with squeezing parametrised by χ', the values of α, ϕ_β and hence χ' are each stochastic variables. As such, the output is the mixed state

$$\hat{\rho} = \int \mathrm{d}\chi' p(\chi') \hat{S}(\chi') |0\rangle |0\rangle \langle 0| \langle 0| \hat{S}^\dagger(\chi') \tag{10}$$

where $p(\chi')$ gives the probability density for the stochastic parameter χ'. Thus, the state is only approximately Gaussian for small noise, with the approximation becoming exact in the limit of no noise.

The term *Gaussian* [2, 24] refers to continuous variable states that can be fully defined by the first two statistical moments of the bosonic or quadrature field operators [25, 26]. First moments can be arbitrarily tuned through local unitary operations, which do not influence any quantity related to entanglement or mixedness [27]. In general, and throughout this work, the first moments can be set to 0 without loss of generality. Displacements or modulations of the input states can be modeled via our set-up by considering heterodyne detection of the arm of the entanglement not sent through the channel. This projects onto coherent states with their displacements in the amplitude and/or phase direction. Thus we do not lose generality by our analysis focusing solely on the covariance matrix of the output state. Thus we focus our analysis only with the covariance matrix of the output state.

The output state (5) covariance matrix is,

$$\Sigma_{\mathrm{out}(4\times4)} = \left\langle \begin{pmatrix} A & C \\ C^T & B \end{pmatrix} \right\rangle \tag{11}$$

where,

$$A = B = \begin{pmatrix} \frac{1+\tanh r'^2}{1-\tanh r'^2} & 0 \\ 0 & \frac{1+\tanh r'^2}{1-\tanh r'^2} \end{pmatrix} \tag{12}$$

$$C = \begin{pmatrix} -\frac{2\tanh r'}{1-\tanh r'^2}\cos(\phi_\beta) & \mathscr{C} \\ \mathscr{C} & \frac{2\tanh r'}{1-\tanh r'^2}\cos(\phi_\beta) \end{pmatrix} \tag{13}$$

$$\mathscr{C} = 2(\cosh r')^{-2} \sum_N (N+1)(\tanh r')^{2N+1} \sin(\phi_\beta) \tag{14}$$

where $C = C^T$. We now employ a small-angle approximations for the noise terms ϕ_j to approximate $\tanh r'$ and $e^{i\phi_\beta}$ in order to establish an analytical expression for the unitary averaging model in the low noise limit. If we assume the individual random phases ϕ_j are independent Gaussian parameters with mean zero and variance v, the expectation values within the covariance matrix can be approximated as

$$\langle \tanh r' \rangle \approx \left(1 - \left(\frac{v}{2} - \frac{v}{2n}\right)\right) \tanh r, \tag{15}$$

$$\langle \cos(\phi_\beta) \rangle \approx \cos\left(\sqrt{\frac{v}{n}}\right) \tag{16}$$

where we have assumed $v \ll 1$ and

$$\left\langle \frac{2\tanh r'}{1-\tanh r'^2}\cos(\phi_\beta) \right\rangle \approx \frac{2\left\langle \tanh r' \right\rangle}{1-\langle \tanh r' \rangle^2} \langle \cos(\phi_\beta) \rangle \tag{17}$$

We compute these analytic approximations and the numerical simulations of the exact covariance matrix (given by Equations 11-13) and analyse the success probability, purity, output squeezing, and the entanglement both with and without applying UA. Note that $\mathscr{C}$ (Eq.14) does not contribute to the average covariance matrix as the individual stochastic phases ϕ_j are independent Gaussian parameters with mean zero. This provides insights into how our protocol protects the channel against stochastic phase noise. Numerical simulations are performed using *Mathematica*, where multiple samples of covariance matrices are considered, each subject to Gaussian, independent, stochastic phase noise with mean zero and variance v. This analysis assumes Gaussianity. In the appendix we explore this approximation by explicitly calculating the 4th moments and comparing them to the Gaussian predictions.

Squeezing factor(r)	Input squeezing	Output squeezing ($n=1$)	Output squeezing ($n=5$)
0.5	4.34	4.09	4.27
1	8.69	6.84	8.17
1.2	10.43	6.87	9.39
1.5	12.03	6.16	10.43
2	17.38	2.49	9.03

Table I: The two-mode squeezing here is reported in decibels. Comparing input to output squeezing. The 'r' value determines the input squeezing. The $n = 1$ case gives the original channel output squeezing (without averaging), and the $n = 5$ case shows the improvement with modest correction (with UA) while the variance is 0.01.

IV. PURITY, SQUEEZING AND ENTANGLEMENT

In realistic systems, phase fluctuations will act to diminish the achieved squeezing and make the state no longer minimum uncertainty [28]. Our protocol has the

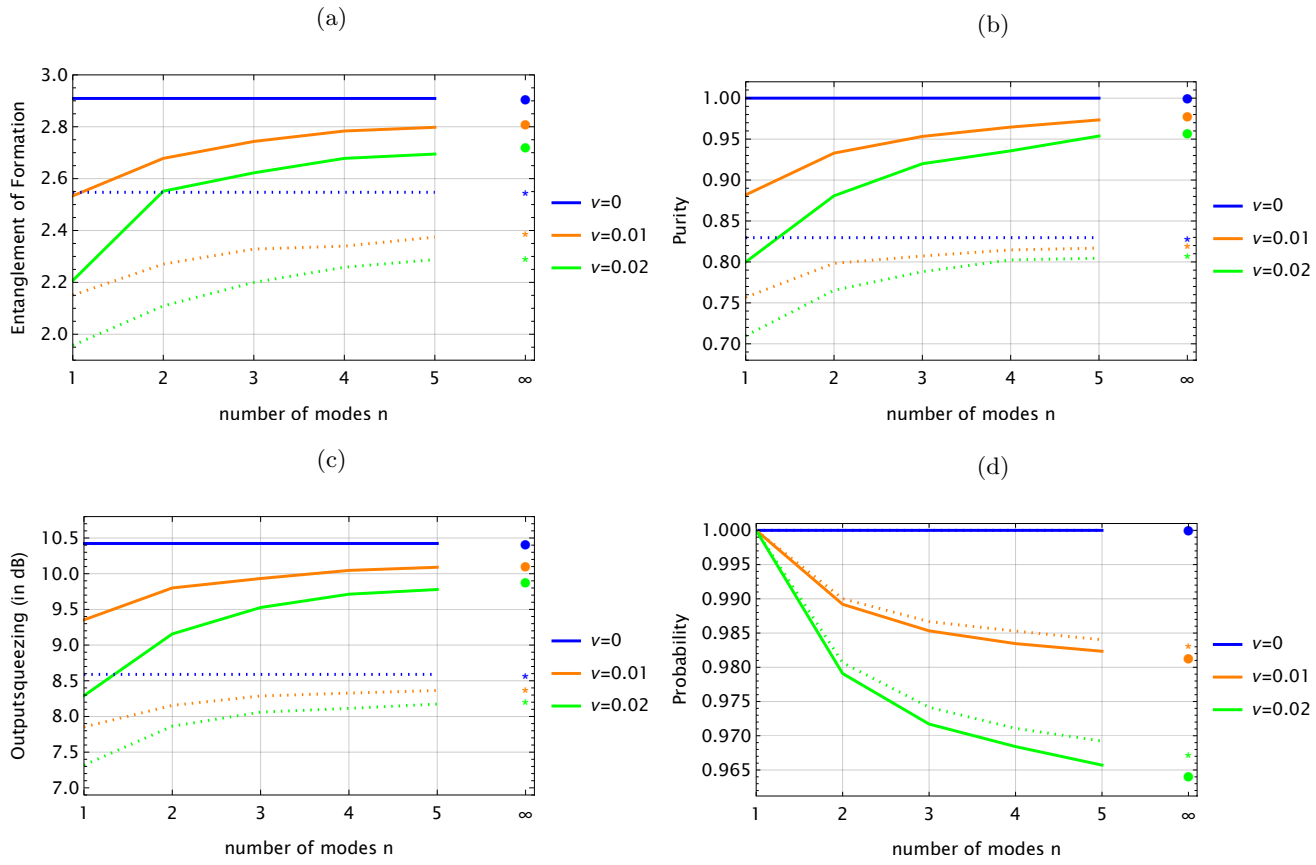

Figure 2: Entanglement, purity and output squeezing improvements when applying unitary averaging to the two-mode squeezed vacuum state with success probability. 2a EoF is maximum with zero-noise level. As the level of noise increases, our protocol progressively transmits more entanglement with the number of modes. 2b Purity is at its peak in a noise-free scenario. As the level of noise increases, our protocol systematically enhances purity with higher number of modes. 2c Similarly, output squeezing is same as input squeezing in noise-free region. The effectiveness of output squeezing improves with higher number of modes with averaging. It is worth noting that the protocol does not lead to squeezing degradation as purity increases. In 2a, 2b & 2c, the results display numerical data both with (dotted upper blue ($\nu = 0$), dotted middle orange ($\nu = 0.01$) and dotted lower green ($\nu = 0.02$) lines) and without (solid blue upper lines ($\nu = 0$), solid orange middle lines ($\nu = 0.01$), solid green lower lines ($\nu = 0.02$)) loss for both practical and asymptotic limit while the input squeezing is 10.4 dB and loss of 10%. 2d gives the probability of success when averaging over only few modes and in the asymptotic limit with input squeezing 10.4 dB. In the appendix, we showed numerical and analytical results are in perfect agreement.

ability to address the issues by effectively lowering the phase noise leading to simultaneously improving purity, squeezing and entanglement through a noisy channel. We are modelling this with the stochastic phases which vary from shot-to-shot.

Measuring the variances of the output state, given its approximate Gaussian nature, serves as a comprehensive means to assess both output squeezing and purity [2, 24]. For a Gaussian state the product of uncertainties is directly related to the purity in the resultant state. Table I clearly illustrates the significant enhancement in squeezing achieved through the channel when utilising the passive averaging protocol. Of particular note is that the maximum possible output two-mode squeezing without averaging ($n = 1$) is significantly lower than the maximum output squeezing that can be achieved with averaging ($n = 5$).

Quantifying entanglement is a non-trivial task as various measures have been defined with distinct operational meanings [27, 29–32]. Here we use the Gaussian entanglement of formation (EoF), which is valued for its important physical significance in quantum technologies [33] because it aligns with the entanglement cost [34]. We utilise the general formula detailed in Reference [31] to upper bound the level of entanglement present in our output state. It represents an analytical upper bound for entanglement of formation of general two-mode Gaussian states. However, we note that we cannot rule out that our measure over estimates the EoF by a small amount as it treats our approximately Gaussian output state as

being exactly Gaussian. The EoF, purity and squeezing are plotted with number of modes n in Fig.2. This shows the practical advantages of the model with significant improvements in the output squeezing, purity and EoF, even for modest n. The output squeezing is seen to increase by 1.5 to 2 dB even for a single extra channel ($n = 2$). Further improvement is seen with larger n. Given that purity and entanglement are interlinked, the channel yields a significant improvement in the resulting entanglement.

We have also calculated the probability of successfully heralding on the vacuum state necessary to produce the lower noise, higher entangled state. The resulting probability scaling is shown in Figure **??**. These show that the probability cost to yield the significant improvements in entanglement, purity and squeezing from the channel are only modest, with at worst a 96.5% chance of successfully heralding on the desired vacuum state, low noise limit we are primarily concerned with here. Importantly, the probability remains at a useful level even in the large n limit and large noise, whilst maintaining non-zero entanglement as shown in the appendix. Note that the level of phase noise will vary depending on the particular experimental situation. To maintain consistency, we ensure phase noise is uniform across all plots in the main text. We have included results with high phase noise in the appendix, thus covering a representative range of situations.

V. LOSS ERRORS

Loss within the channel and vacuum detectors is modelled as beamsplitters before each element. These beamsplitters mix the channel with the vacuum with transmission $\sqrt{1-\gamma}$ and hence a loss probability γ [35, 36]. This operation, however, can be commuted through the entire transformation applied to the input mode until it is the first operation acting on the input state, provided we consider the loss to act on all modes equally, including both modes of the conditional output state. Hence, distributed loss acting within the channel and the heralding detectors is equivalent to the same loss acting only on the initial state. Note that as most inputs are in the vacuum it only looks like loss acting on the input two mode squeezed state. In Fig.2 we include plots with 10% loss and observe that the protocol still mitigates the effects of phase noise. This tells us that loss in the vacuum projection detectors and in the initial state do not impact the ability to correct the phase noise. We note that we have made the standard assumption that the phase noise and loss in our channel can be treated separately.

VI. CONCLUSION

Our protocol can be effectively implemented within state-of-the-art quantum communication and computing platforms, as it relies on readily available Gaussian states, linear optics setups, and vacuum projection, all commonly found in various practical bosonic systems.

In summary, we have presented a passive unitary averaging scheme with vacuum detection acting on one arm of a two-mode squeezed state. We found it successfully limits the effect of phase noise within the channel. Over an order of magnitude of noise reduction was achieved surprisingly with an increase in squeezing as well as purity, and enhancing levels of entanglement available in realistic systems. We expect that the UA techniques described here will find immediate applications in quantum communications and optical quantum computing schemes.

VII. ACKNOWLEDGEMENT

We thank Deepesh Singh for helpful discussion about unitary averaging. SNS expresses gratitude to Giacomo Pantaleoni, Fumiya Hanamura and Takaya Matsuura for their discussions on Gaussian states. SNS was supported by the Sydney Quantum Academy, Sydney, NSW, Australia. This work was partially supported by the Australian Research Council Centre of Excellence for Quantum Computation and Communication Technology (Project No.CE110001027).

Appendix A: Purity and output squeezing formula

Added new section:

The unitary averaged output state is,

$$|\psi_{out}\rangle = \frac{1}{\mathbf{N}} (\cosh r)^{-1} \sum_N (-1)^N [e^{i\phi_\beta} \tanh r']^N |N, N\rangle \tag{A1}$$

where $\mathbf{N}$ is a normalisation constant and the normalisation constant for the output state (A1) is,

$$\mathbf{N} = \frac{\cosh r'}{\cosh r} \tag{A2}$$

Then we present output-squeezing and purity of Eq.(A1) by calculating the variance and covariance of the output state.

The output squeezing is given by,

$$\text{output-squeezing} = \left(\frac{1+\tanh r'^2}{1-\tanh r'^2}\right) - \left(\frac{2\tanh r'}{1-\tanh r'^2}\cos(\phi_\beta)\right) \tag{A3}$$

In analytical approximation,

$$\text{output-squeezing} \approx \left(\frac{1+\left(\left(1-\left(\frac{v}{2}-\frac{v}{2n}\right)\right)\tanh r\right)^2}{1-\left(\left(1-\left(\frac{v}{2}-\frac{v}{2n}\right)\right)\tanh r\right)^2}\right) - \left(\frac{2\left(\left(1-\left(\frac{v}{2}-\frac{v}{2n}\right)\right)\tanh r\right)}{1-\left(\left(1-\left(\frac{v}{2}-\frac{v}{2n}\right)\right)\tanh r\right)^2}\cos\left(\sqrt{\frac{v}{n}}\right)\right) \tag{A4}$$

The output-anti squeezing is defined as,

$$\text{output-antisqueezing} = \left(\frac{1+\tanh r'^2}{1+\tanh r'^2}\right) - \left(\frac{2\tanh r'}{1-\tanh r'^2}\cos(\phi_\beta)\right) \tag{A5}$$

The purity is defined as,

$$\text{Purity} = \frac{1}{\sqrt{(\text{output-squeezing})(\text{output-antisqueezing})}} \tag{A6}$$

We use the above formulae to present purity and output-squeezing in the main text in the fig.2 as well as all plots in the Appendix C.

Appendix B: Passive unitary averaging with loss on CV systems

In the main text, we operate under the assumption of zero channel loss within the model. We clarify in the main text that loss occurring within the channel or detectors is equivalent to loss within the initial state. As most inputs are in the vacuum, it looks like loss acting only on the two-mode squeezed vacuum state. This equivalence is true provided there is the same amount of end-to-end loss, $1-\eta$, on all modes. If this is true then the output when loss is distributed through the circuit is equivalent to the output when the same loss is applied to the input state, which is then propagated through a lossless circuit. In this section, we calculate the output for the two mode squeezed vacuum state which undergoes loss, and then passes through the passive, linear optical unitary averaging scheme. For the sake of mathematical simplicity, we consider the case where the mode $\hat{a}_1$ undergoes loss. The calculation of the covariance matrix is easier when approached through Heisenberg picture. The resulting channel transmissivity is η.

In our case, the two-mode squeezer acts on the modes labeled $\hat{a}_0$ and $\hat{a}_1$. Then, the transmitted mode becomes,

$$\hat{a}_1' = \sqrt{\eta}\hat{a}_1 + \sqrt{1-\eta}v_1 \tag{B1}$$

where v_1 is vacuum noise of mode $\hat{a}_1$. After passing through the loss, interferometer and heralding on the last $(n-1)$ modes, the output state is

$$|\psi_{\text{out}}\rangle = \left(\otimes_{j=2}^{n}\langle 0|_j\right)\hat{L}_1\hat{U}\hat{S}(r)|0\rangle|0\rangle\otimes|0\rangle^{\otimes(n-1)} \tag{B2}$$

where $\hat{L}_1$ is loss acting on mode $\hat{a}_1$, $\hat{U} = (\hat{H}^\dagger * \hat{R}(\theta) * \hat{H})_{n\times n}$, $\hat{H}$ is the Hadamard transforms acting as the encoding and decoding circuits, and $\hat{R}(\theta)$ implements stochastic phase transformations on each mode, representing the noise.

The output state is,

$$|\psi_{\text{out}}\rangle = \frac{1}{\mathbf{N}}(\cosh r)^{-1}\sum_{N=0}^{\infty}\sum_{K=0}^{N}\frac{\sqrt{N!}}{\sqrt{K!}\sqrt{(N-K)!}}(-1)^N(\tanh r)^N(\alpha e^{i\phi_\beta})^{N-K}\eta^{\frac{N-K}{2}}(1-\eta)^{\frac{K}{2}}|N,N-K,K\rangle \tag{B3}$$

where $\mathbf{N}$ is a normalisation constant related to probability of success, K is the lossy mode and $\alpha e^{i\phi_\beta} = \frac{e^{i\phi_1}+e^{i\phi_2}+\ldots+e^{i\phi_n}}{n}$.

The normalisation constant for the output state (B3) is,

$$\mathbf{N} = \sqrt{\frac{(\text{sech}\, r)^2}{-1+(1+(-1+|\alpha e^{i\phi_\beta}|^2)\eta)(\tanh r)^2}} \tag{B4}$$

We again use the covariance matrix formalism [2, 25] to characterise the output state after introducing loss into the input two-mode squeezed vacuum state. We present the numerical results with loss in the main text in Fig.2.

Appendix C: Several plots showing numerical and analytical agreement

In this section, we present various plots demonstrating the alignment between analytical and numerical results, specifically fitted to showcase advancements in practical technologies. Additionally, we demonstrate the asymptotic nature of our protocol. In Fig.2, we show numerical and analytical results are in perfect agreement in the low noise regime. As the noise level increases, our protocol dynamically increases the transmission of entanglement, purity, and squeezing compared to a noisy channel, with at worst 93% success probability for the noise levels considered, as shown in Figures 2 and 4. Fig.5 shows

how entanglement, purity, output squeezing and success probability change with varying levels of input squeezing with low noise. Entanglement and squeezing initially increase with input squeezing but diminish at higher input squeezing levels, although it still improves with an increased number of modes. Purity decreases as squeezing increases but again improved with a larger number of modes. In Fig.8 we illustrate the robust aspect of our protocol, which remains benifitial even under high squeezing and demonstrate its behaviour when utilising a large number of modes.

Appendix D: Success probability with dark counts

The presence of dark counts in the heralding detectors reduces the probability of success but doe not otherwise affect the quality of the phase noise reduction. When the detector registers events due to dark counts during vacuum detection, these are false negatives and hence the success probability decreases. We can thus account for the presence of dark counts via:

$$\text{PSuccess} = (1-\epsilon)^{n-1} \times \text{Probability} \tag{D1}$$

The impact of dark counts on the success probability of our model are shown in (Fig.7).

Appendix E: Gaussian character of the output state.

Added new section: In order to estimate the non-Gaussianity of our output states we study the affect on the 4th order moments, with and without error averaging, and compare them with the expected results for Gaussian states. This is shown in the following. The conclusion is that modest levels of non-Gaussianity ($< 10\%$) can arise after averaging, however we note that Gaussian optimality in many situations (e.g. CVQKD key rates and Gaussian entanglement of formation) mean performance is lower bounded by assuming a Gaussian state.

The fourth moment of our output state which are

$$\langle X_A^4 \rangle = -\frac{(\operatorname{sech} r')^2(1+\tanh r'^2)}{(-1+\tanh r'^2)^3} \tag{E1}$$

$$\langle X_A^2 X_B^2 \rangle = -\frac{(\operatorname{sech} r')^2(1+10\tanh r'^2+\tanh r'^4)}{(-1+\tanh r'^2)^3} \times \left(\frac{e^{i\phi}+e^{-i\phi}}{2}\right) \tag{E2}$$

When the phase noise is low, the relationship $\langle X_A^4 \rangle = 3(\langle X_A^2 \rangle)^2$, $\langle X_A^2 X_B^2 \rangle = 2(\langle X_A^2 \rangle)^2 + (\langle X_A X_B \rangle)^2$ approximately aligns with the second moment. From Fig.6, it is evident that the relationship differs by less than 10%, indicating that the state is approximately Gaussian.

[1] H.-A. Bachor and T. C. Ralph, A guide to experiments in quantum optics, (3rd Edition Wiley, New York, 2019).

[2] C. Weedbrook, S. Pirandola, R. García-Patrón, N. J. Cerf, T. C. Ralph, J. H. Shapiro, and S. Lloyd, Gaussian quantum information, Reviews of Modern Physics **84**, 621 (2012).

[3] A. Furusawa, J. L. Sørensen, S. L. Braunstein, C. A. Fuchs, H. J. Kimble, and E. S. Polzik, Unconditional quantum teleportation, Science **282**, 706 (1998).

[4] F. Grosshans, G. Van Assche, J. Wenger, and et al., Quantum key distribution using gaussian-modulated coherent states, Nature **421**, 238 (2003).

[5] A. P. Lund, A. Laing, S. Rahimi-Keshari, T. Rudolph, J. L. O'Brien, and T. C. Ralph, Boson sampling from a gaussian state, Physical review letters **113**, 100502 (2014).

[6] C. S. Hamilton, R. Kruse, L. Sansoni, S. Barkhofen, C. Silberhorn, and I. Jex, Gaussian boson sampling, Physical Review Letters **119**, 170501 (2017).

[7] H.-S. Zhong, H. Wang, Y.-H. Deng, M.-C. Chen, L.-C. Peng, Y.-H. Luo, J. Qin, D. Wu, X. Ding, Y. Hu, P. Hu, X.-Y. Yang, W.-J. Zhang, H. Li, Y. Li, X. Jiang, L. Gan, G. Yang, L. You, Z. Wang, L. Li, N.-L. Liu, C.-Y. Lu, and J.-W. Pan, Quantum computational advantage using photons, Science **370**, 1460 (2020).

[8] L. S. Madsen, F. Laudenbach, M. F. Askarani, F. Rortais, T. Vincent, J. F. F. Bulmer, F. M. Miatto, L. Neuhaus, L. G. Helt, M. J. Collins, A. E. Lita, T. Gerrits, S. W. Nam, V. D. Vaidya, M. Menotti, I. Dhand, Z. Vernon, N. Quesada, and J. Lavoie, Quantum computational advantage with a programmable photonic processor, Nature **606**, 75 (2022).

[9] R. J. Marshman, A. P. Lund, P. P. Rohde, and T. C. Ralph, Passive quantum error correction of linear optics networks through error averaging, Physical Review A **97**, 022324 (2018).

[10] M. K. Vijayan, A. P. Lund, and P. P. Rohde, A robust w-state encoding for linear quantum optics, Quantum **4**, 303 (2020).

[11] R. J. Marshman, D. Singh, A. P. Lund, and T. C. Ralph, Unitary averaging with fault and loss tolerance, arXiv preprint arXiv:2304.14637 (2023).

[12] D. Singh, A. P. Lund, and P. P. Rohde, Optical cluster-state generation with unitary averaging, arXiv preprint arXiv:2209.15282 (2022).

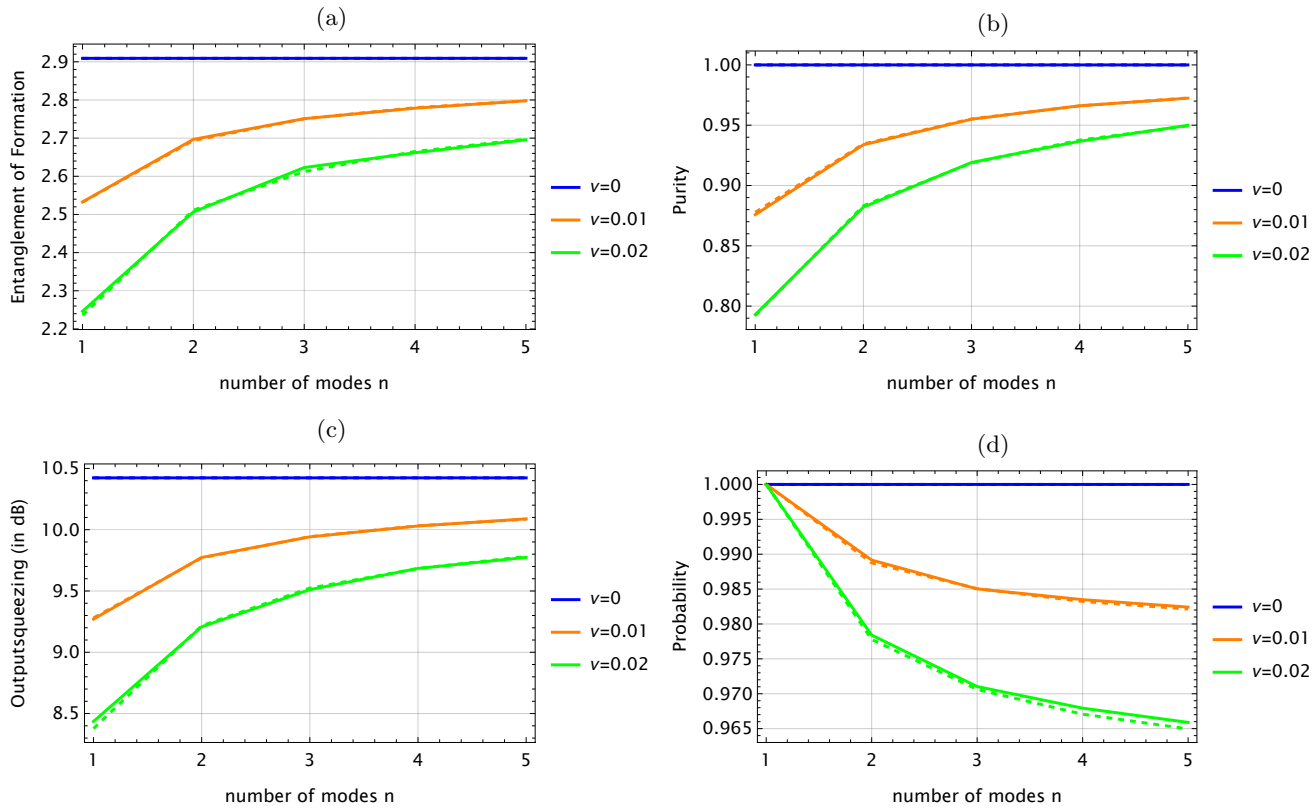

Figure 3: Entanglement, purity and output squeezing improvements with success probability when applying unitary averaging to the two-mode squeezed vacuum state. 3a EoF is maximum with zero-noise level. As the level of noise increases, our protocol progressively transmits more entanglement with the number of modes. 3b Purity is at its peak in a noise-free scenario. As the level of noise increases, our protocol systematically enhances purity with higher number of modes. 3c Similarly, output squeezing is same as input squeezing in noise-free region. The effectiveness of output squeezing improves with higher number of modes with averaging. It is worth noting that the protocol does not lead to squeezing degradation as purity increases. In 3a, 3b & 3c, the numerical (solid lines) and analytical (dotted lines) results are in perfect agreement with input squeezing 10.4 dB. 3d gives the probability of success when averaging over only few modes. The numerical (solid blue upper lines ($\nu = 0$), solid orange middle lines ($\nu = 0.01$), solid green lower lines ($\nu = 0.02$)) and analytical (dashed blue upper lines ($\nu = 0$), dashed orange middle lines ($\nu = 0.01$), dashed green lower lines ($\nu = 0.02$)) results are in perfect agreement with input squeezing 10.4 dB.

[13] J. Fiurášek, Gaussian transformations and distillation of entangled gaussian states, Physical review letters **89**, 137904 (2002).

[14] G. Giedke and J. I. Cirac, Characterization of gaussian operations and distillation of gaussian states, Physical Review A **66**, 032316 (2002).

[15] J. Niset, J. Fiurášek, and N. J. Cerf, No-go theorem for gaussian quantum error correction, Physical review letters **102**, 120501 (2009).

[16] P. K. Lam, T. C. Ralph, B. C. Buchler, D. E. McClelland, H.-A. Bachor, and J. Gao, Optimization and transfer of vacuum squeezing from an optical parametric oscillator, Journal of Optics B: Quantum and Semiclassical Optics **1**, 469 (1999).

[17] S. P. Kish, P. Gleeson, P. K. Lam, and S. M. Assad, Comparison of discrete variable and continuous variable quantum key distribution protocols with phase noise in the thermal-loss channel, Quantum **8**, 1382 (2024).

[18] Z. Y. Ou, S. F. Pereira, H. J. Kimble, and K. C. Peng, Realization of the einstein-podolsky-rosen paradox for continuous variables, Phys. Rev. Lett. **68**, 3663 (1992).

[19] A. Franzen, B. Hage, J. DiGuglielmo, J. Fiurasek, and R. Schnabel, Experimental demonstration of continuous variable purification of squeezed states, Physical review letters **97**, 150505 (2006).

[20] J. Fiurášek, P. Marek, R. Filip, and R. Schnabel, Experimentally feasible purification of continuous-variable entanglement, Physical Review A **75**, 050302 (2007).

[21] M. Lassen, L. S. Madsen, M. Sabuncu, R. Filip, and U. L. Andersen, Experimental demonstration of squeezed-state quantum averaging, Physical Review A **82**, 021801 (2010).

[22] B. L. Schumaker and C. M. Caves, New formalism for two-photon quantum optics. ii. mathematical foundation and compact notation, Physical Review A **31**, 3093 (1985).

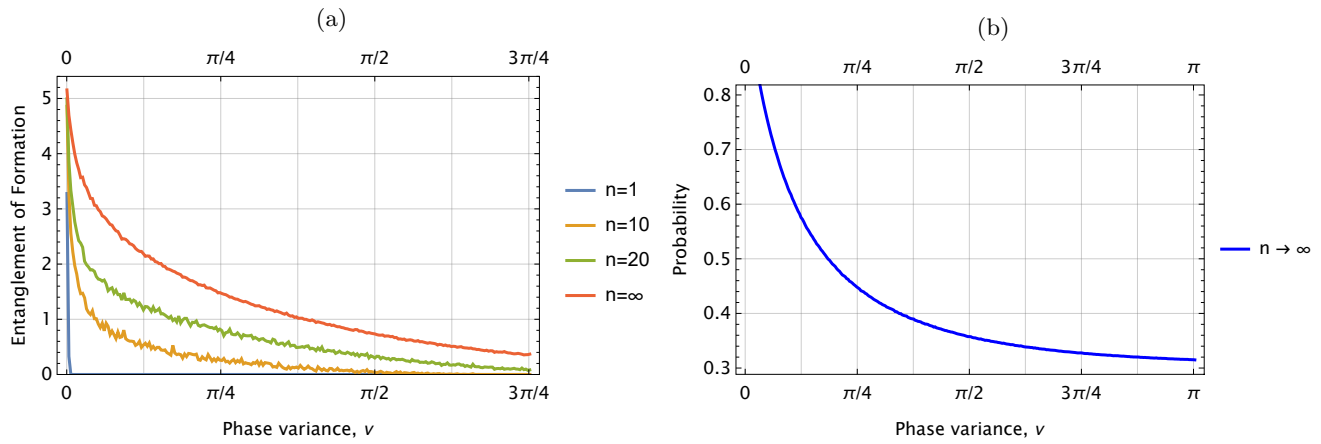

Figure 4: Entanglement and probability in the asymptotic limit with input squeezing 10.4 dB. 4a Entanglement is enhancing with increased phase variance $n \to \infty$ limit. Lower gray blue line is for $n = 1$, above lower orange line is for $n = 10$, second last green line is for $n = 20$ and the upper red line is for $n = \infty$. 4b Probability is non-zero with sufficiently high noise in the asymptotic n limit.

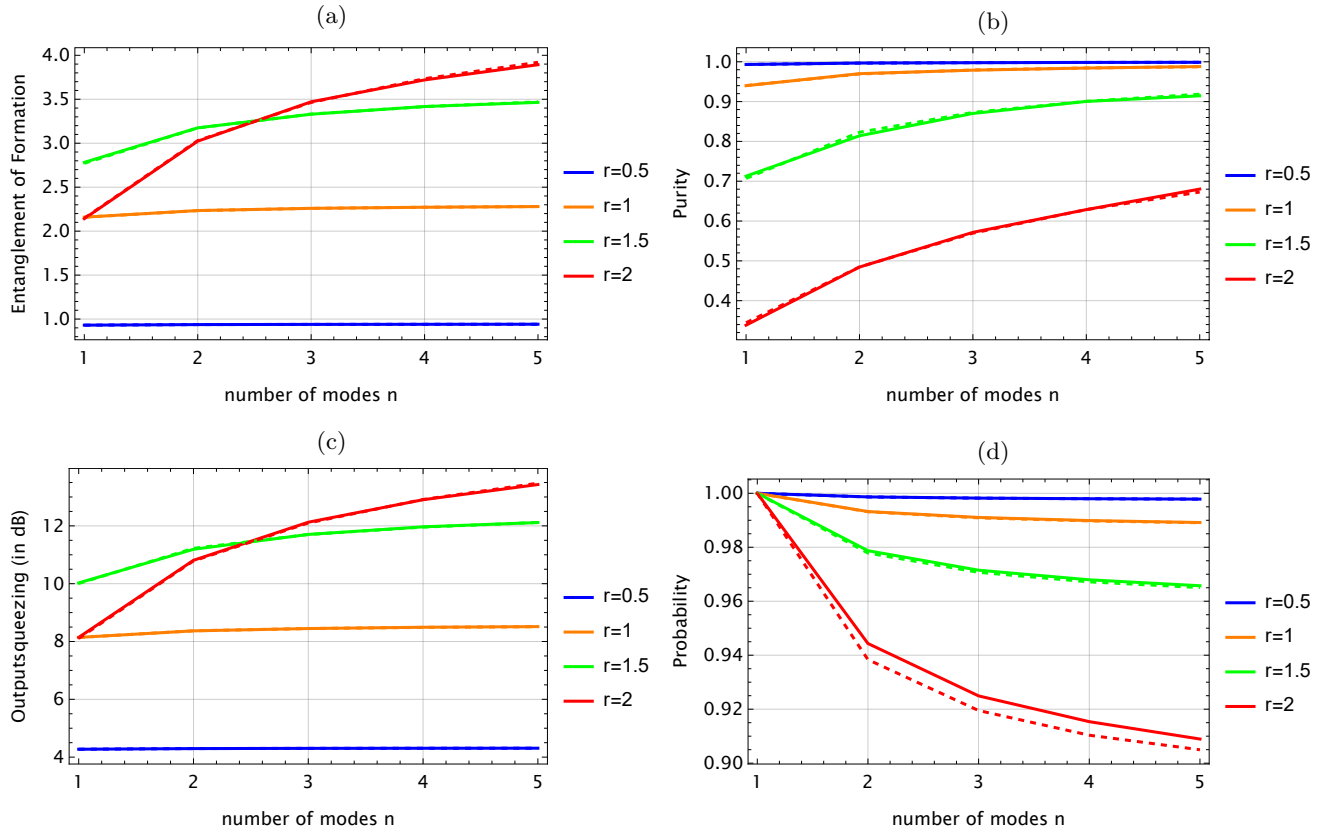

Figure 5: Entanglement, purity and output squeezing varies alongside the success probability when applying unitary averaging to the two-mode squeezed vacuum state with varying levels of input squeezing in the low noise limit. 5a EoF began to decline at input squeezing $r = 2$. 5b Purity decays with the increasing input squeezing and interestingly even at the high level of input squeezing, the output state is not completely mixed. 5c Similarly, output squeezing started decreasing after reaching input squeezing $r = 1.5$. In 5a, 5b & 5c, The numerical (solid lines) and analytical (dashed lines) results are in perfect agreement with noise 0.01. 5d Numerical Probability looses agreement with analytical probability from $r = 2$ (lower red solid and dashed lines) with noise 0.01.

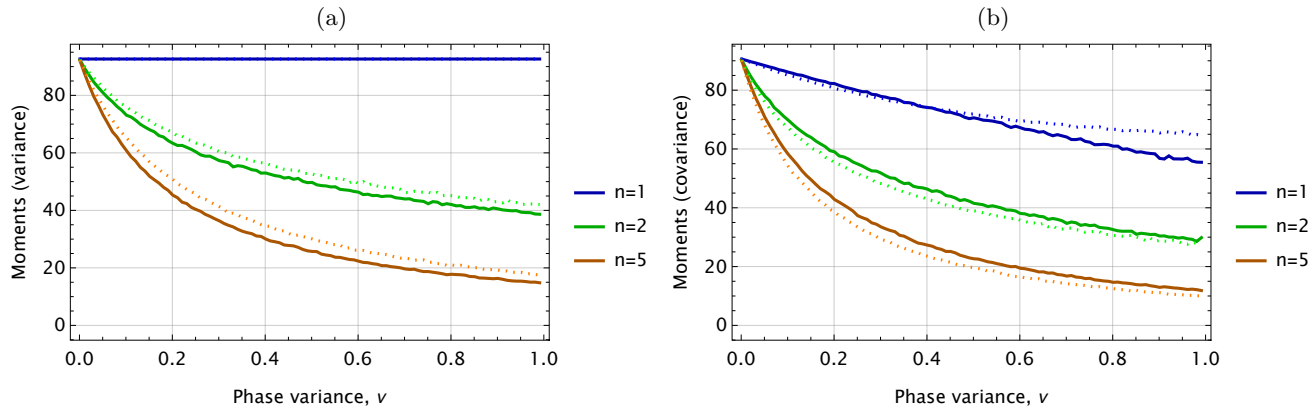

Figure 6: 6a, 6b Gaussian moments with phase noise when input squeezing is 10.4 dB. Solid lines (solid blue upper lines ($n = 1$), solid green middle lines ($n = 2$), solid orange lower lines ($n = 5$)) represents the 4th order moment, while the dotted line (dotted upper blue ($n = 1$), dotted middle green ($n = 2$) and dotted lower orange ($n = 5$) lines) shows the relationship with the 2nd order moment. Both the moments differ by less than 10% .

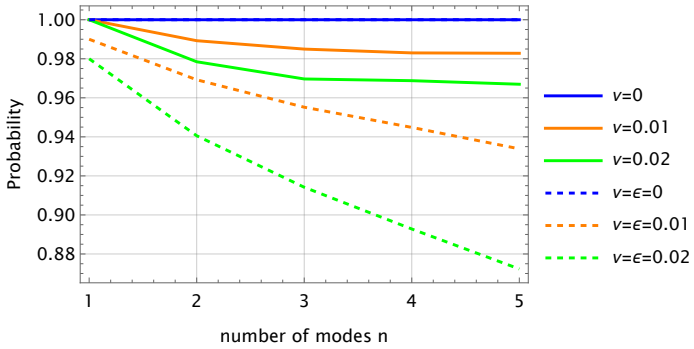

Figure 7: probability of success when averaging over only few modes with input squeezing 10.4 dB. ν is the variance and ϵ is the dark count. Solid lines (solid blue upper lines ($\nu = 0$), solid orange middle lines ($\nu = 0.01$), solid green lower lines ($\nu = 0.02$)) represent channel with only phase noise and the dotted lines (dotted upper blue ($\nu = 0$), dotted middle orange ($\nu = 0.01$) and dotted lower green ($\nu = 0.02$) lines) represent both with phase noise and dark counts.

[23] A. I. Lvovsky, Squeezed light, Photonics: Scientific Foundations, Technology and Applications **1**, 121 (2015).

[24] A. Ferraro, S. Olivares, and M. G. Paris, Gaussian states in continuous variable quantum information, arXiv preprint quant-ph/0503237 (2005).

[25] A. Serafini, *Quantum continuous variables: a primer of theoretical methods* (CRC press, 2023).

[26] N. C. Menicucci, S. T. Flammia, and P. van Loock, Graphical calculus for gaussian pure states, Physical Review A **83**, 042335 (2011).

[27] R. Horodecki, P. Horodecki, M. Horodecki, and K. Horodecki, Quantum entanglement, Reviews of modern physics **81**, 865 (2009).

[28] D. F. Walls, Squeezed states of light, nature **306**, 141 (1983).

[29] V. Vedral, M. B. Plenio, M. A. Rippin, and P. L. Knight, Quantifying entanglement, Physical Review Letters **78**, 2275 (1997).

[30] W. P. Bowen, R. Schnabel, P. K. Lam, and T. C. Ralph, Experimental characterization of continuous-variable entanglement, Physical review A **69**, 012304 (2004).

[31] S. Tserkis and T. C. Ralph, Quantifying entanglement in two-mode gaussian states, Physical Review A **96**, 062338 (2017).

[32] S. Tserkis, S. Onoe, and T. C. Ralph, Quantifying entanglement of formation for two-mode gaussian states: Analytical expressions for upper and lower bounds and numerical estimation of its exact value, Physical Review A **99**, 052337 (2019).

[33] E. Chitambar and G. Gour, Quantum resource theories, Reviews of modern physics **91**, 025001 (2019).

[34] P. M. Hayden, M. Horodecki, and B. M. Terhal, The asymptotic entanglement cost of preparing a quantum state, Journal of Physics A: Mathematical and General **34**, 6891 (2001).

[35] V. V. Albert, K. Noh, K. Duivenvoorden, D. J. Young, R. Brierley, P. Reinhold, C. Vuillot, L. Li, C. Shen, S. Girvin, *et al.*, Performance and structure of single-mode bosonic codes, Physical Review A **97**, 032346 (2018).

[36] V. V. Albert, Bosonic coding: introduction and use cases, arXiv preprint arXiv:2211.05714 (2022).

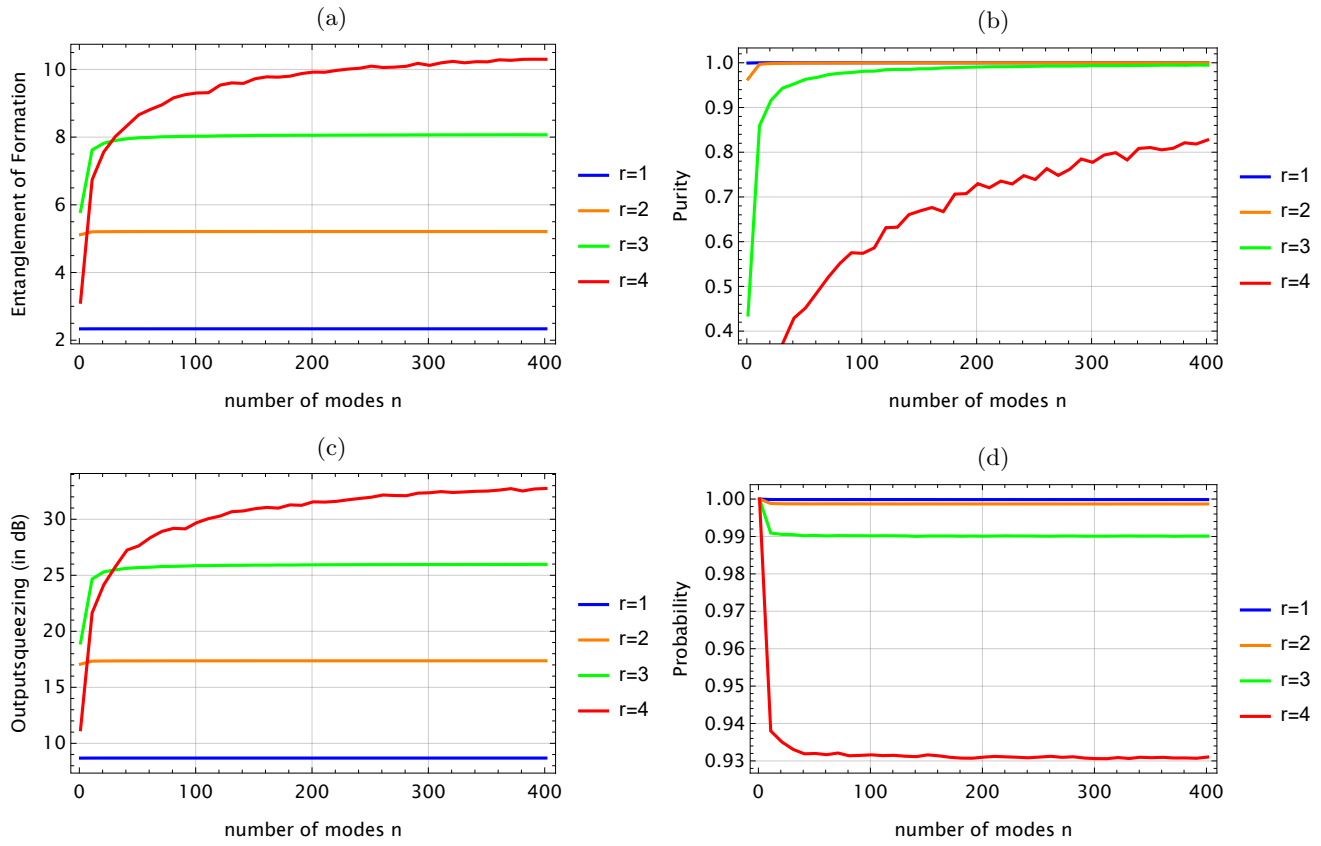

Figure 8: Entanglement, purity and output squeezing varies alongside the success probability when applying unitary averaging to the two-mode squeezed vacuum state with varying levels of input squeezing in the asymptotic limit with noise 0.01. 8a & 8c EoF and output squeezing behave similarly with the higher number of modes with high input squeezing. 8b Purity increases with the number of modes and getting saturated with the higher number of modes. 8d Probability of success drops massively for input squeezing $r = 4$, and getting saturated with higher n.